Comparison Of Velocity & Temperature Measurements In The Cfff Aerodynamic Duct With Flow Field Model Calculations

Author(s): W. W. Wilson, J. P. Singh, F. Y. Yueh, A. George, R. L. Cook, J. J. Lee and J. T. Lineberry

Session Name: Instrumentation & Diagnostics

SEAM: 31 (1993)

SEAM EDX URL: https://edx.netl.doe.gov/dataset/seam-31

EDX Paper ID: 1657

COMPARISON OF VELOCITY AND TEMPERATURE MEASUREMENTS IN THE CFFF AERODYNAMIC DUCT WITH FLOW FIELD MODEL CALCULATIONS

W.W. WILSON, JAGDISH P. SINGH, F.Y. YUEH, A. GEORGE AND ROBERT L. COOK

Diagnostic Instrumentation and Analysis Laboratory
Mississippi State University
Mississippi State, MS 39762

and

J.J. LEE AND J.T. LINEBERRY

Energy Conversion Research and Development Programs
The University of Tennessee Space Institute
Tullahoma, TN 37388

ABSTRACT

This paper reports measurements of velocity and temperature in the topping cycle environment found in the aerodynamic duct of the Coal-Fired Flow Facility (CFFF). Details of the measurement methods are given. Also, the measurements are compared with ideal thermodynamic expansion calculations and a multidimensional gas dynamic model of the velocity and temperature within the duct. Discussions of data analyses and numerical model simulations of the flow field within the CFFF LMF supersonic aerodynamic duct are provided. The measured temperature and flow velocity are lower than expected and more representative of the subsonic flow. The possible origin of this result is discussed. These results and other measurements in the aerodynamic duct carried out since 1992 demonstrate that on-line optical measurements of an MHD coal-combustion plasma can be made in the highly stressed, thermodynamic environment that is typical to that existing in the coal-fired MHD generator.

INTRODUCTION

The importance of directly measuring performance parameters such as temperature and flow velocity for the safe, efficient and reliable operation of an MHD power plant has been discussed previously by Kumar and Cook[1]. In general, measurement of temperature, gas velocity, potassium atom number density, electron number density, average particle size, and concentrations of certain molecular species allow for characterization of the plasma and gas stream and provide the means to monitor, control, and optimize the systems operation and to diagnose potential problems. In particular, monitoring these performance parameters are essential to:

- enable optimum control of the MHD power plant;
- properly interpret gross behavior of the power system;
- pinpoint the origin of a power shortfall;
- provide early warning of potential problems;
- maintain high plant efficiency;
- maintain operational safety; and
- maintain system longevity through preventive maintenance.

Measurements of performance parameters are particularly important in the topping cycle region of an MHD power plant. Although the gas stream environment inside a coal-fired MHD power train is rather hostile, optical-based measurement systems can provide nonintrusive, real-time values of the desired performance/control parameters.

This paper reports on the measurement of velocity and temperature in the topping cycle environment found in the aerodynamic duct of the Coal-Fired Flow Facility (CFFF) which is located at the University of Tennessee Space Institute (UTSI). These results will be compared with ideal thermodynamic expansion calculations and a multidimensional gas dynamic model of the velocity and temperature within the duct. These modeling studies provide a means by which the flow field and heat transfer that develop within the CFFF aerodynamic duct can be viewed. They also form a basis by which the experimental data can be compared and qualified and also the model evaluated. The modeling techniques that were applied in this research to define the flow field have been used in the past to analyze the gas dynamics and heat transfer in various CFFF/UTSI test train components.

The location of the measurements is about 31" from the nozzle throat, (see Figure 1) where the gas stream is about 4.75" wide. The characteristics of the gas stream are typical of the topping cycle region.

The local velocity measurements and the velocity profile reported here were obtained with a laser Doppler velocimeter (LDV) system. This system has been described previously by Wilson, et. al[2,3] and velocity profile measurements in the CFFF diffuser and furnace are described elsewhere.[2-4] The local plasma temperature measurements in the aerodynamic duct were made with a coherent anti-Stokes Raman spectroscopy (CARS) system described in detail by Singh, et al.[5,6] Previous temperature profile measurements in the CFFF diffuser have been previously reported and compared with model calculations.[7] These diagnostic systems developed at Mississippi State University (MSU) by the Diagnostic Instrumentation and Analysis Laboratory (DIAL) where transported and operated from DIAL's 18-wheeler-based mobile instrument laboratory.

To allow for measurements in the topping cycle region special optical access techniques and systems (OATS) have been developed. Details of these systems have been described by Hester and Cook[8] and more recently by Cook and Lineberry.[9] Briefly, these systems provide for remotely changing dirty optical windows and means for removing any slag build-up across the optical port. Figure 2 shows the OATS used at the CFFF aerodynamic duct which provided long-term optical access to the plasma stream. It should be noted that the optical access hole at the gas stream was only about 1 inch in diameter.

CFFF LMF OPERATING CONDITIONS

The experimental data that are presented herein were taken using the MSU OATS in the CFFF LMF test train during two western coal (Montana Rosebud) POC tests of 1993. These tests were: LMF5-F of August '93 which resulted 290 hours of accumulated coal-fired operation of the CFFF; and, LMF5-G of October '93 which achieved 314 accumulated hours of coal-firing.

Both the LDV and the CARS measurements were made during sustained periods of time (hours) during each of these tests in which combustor operation and that of the entire CFFF test train was held stable at its nominal western coal POC operating point. The CFFF LMF western coal POC combustor operating point along with general combustor performance measures are summarized in Table I.

One point which is emphasized concerning the CFFF LMF POC operating point is the use of aqueous solution of K_2CO_3 for seeding the plasma. The liquid of the seed solution allows for fine control of the seeding rate in this system. However, it also tends to quench the combustor flame about 60K below that which is achievable with dry seed.

More detail on CFFF LMF combustor operation for the western coal POC test program can be found in various reference materials and reports on this facility and the POC test program. Particular references which detail operation and performance of the upstream LMF test train and summarize the work of implementation of the OATS into this part of the CFFF are cited in the bibliography as references 9 and 10. These references also provide descriptions on the hardware, components, operation, and history of operation of the CFFF LMF "upstream" test train.

TABLE I

CFFF POC COMBUSTOR OPERATING POINT

Combustor Flows (kg/s):

Coal	0.37
Oil	0.21
Air	1.58
O_2	0.85
Seed	0.12 †

Operating Point Specs:

Oil / Coal	0.57 ††
Stoichiometry	85%
N/O	1.0
Q_{th} Input	18.5 Mw
Seed Fraction	1.0 % †††
K_2 / S	4.02

Adiabatic Flame State: T_{flame} = 2,872 K, P_{comb} = 4.51 Atm

†Aqueous Solution - 47% K_2CO_3 by Mass

†† Fuel Mix is Based on 50:50 per Thermal Input

††† Ratio of Potassium to Total Flow by Mass

VELOCITY AND TURBULENCE MEASUREMENTS

Laser Doppler velocimetry (LDV) measurements were performed in the aerodynamic duct of the Coal Fired Flow Facility at UTSI during LMF5-F August 13-15, 1992. The experiment was done in the forward scatter mode and optical access was provided as illustrated in Figure 2. A schematic of the LDV apparatus used for this experiment is shown in Figure 3.

Laser Doppler velocimeter has been extensively used for the measurement of gas velocity and turbulence level at a given point in gas streams. The technique measures the velocity of small scattering centers by detecting the Doppler shift in the scattered laser light[11]. This is achieved by crossing two focused laser beams. The measurement volume formed by the intersection of laser beams has an ellipsoidal shape. Interference fringes will be produced at the point of beam crossing. Alternative scattering or no scattering of light into the detector will occur as a particle proceeds through the beam intersection. The scattered light will produce a detector current of

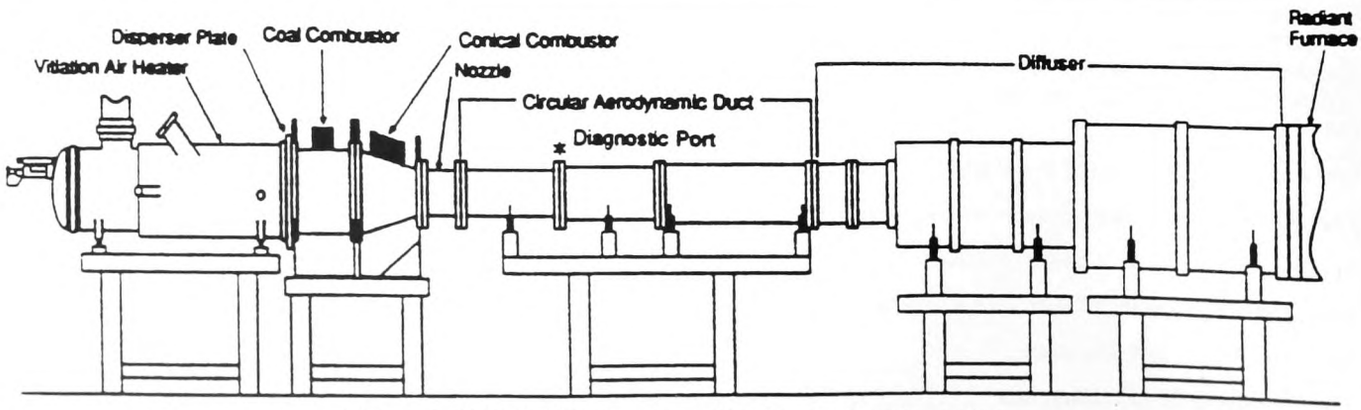

Figure 1. CFFF/UTSI Upstream Flow Train Configuration

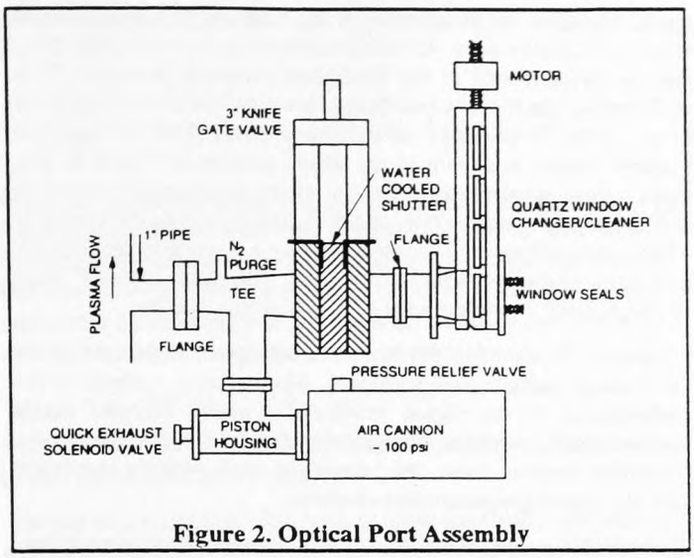

Figure 2. Optical Port Assembly

frequency proportional to the rate at which the particle intercepts the fringes. This Doppler frequency is proportional to the velocity component parallel to the plane defined by the two beams and inversely proportional to the fringe spacing. Different measurement points inside the gas stream are achieved by moving the focusing lens system. The scattered light signal arriving at the detector will be the same regardless of the direction in which the particle travels. This directional uncertainty in the LDV experiments is corrected by shifting the frequency of one of the beams using a Bragg cell. The frequency shift used in this measurement was 40 MHz.

The diameter of the ellipsoidal measurement volume is calculated by the following equation

$$d_m = \frac{4\lambda f}{\pi D E} \tag{1}$$

where λ is the wavelength of the laser (514.5 nm), E is the beam expansion ratio, f is the focal length of the lens and D is the diameter of the laser beam. The transmitting optics used in this experiment consisted of a 9 mm beam spacer, a 3.75X beam expander and a 6" diameter focusing lens having a focal length of 1130 mm. This combination gave a diameter of 132 µm for the measurement volume.

The measurement volume diameter can be related to the length of the measurement volume (l_m) by the following equation:

$$l_m = \frac{d_m}{\tan\kappa} \approx \frac{2 d_m f}{E d} \tag{2}$$

where d_m is the distance between the laser beams entering the lens. For the optical setup used in this study the calculated length of the measurement volume is about 8.8 mm. When the two laser beams cross, they will produce a set of closely spaced, planar interference fringes at the point of crossing. The angle between the two beams can be calculated as

$$\kappa = \tan^{-1}\frac{E d}{2 f} \tag{3}$$

The value of κ calculated for the optical setup for this experiment is 0.856°.

The fringe spacing is given by

$$d_f = \frac{\lambda}{2\sin\kappa} \approx \frac{\lambda f}{E d} \tag{4}$$

In this case, the calculated value for the fringe spacing is 17.23 µm. Since the fringe spacing is known, the velocity of a particle crossing the probe volume is given by

$$U_x = f_D d_f \tag{5}$$

where f_D is the frequency of the Doppler burst. For a measured centerline Doppler burst of frequency 55 MHz, we will have a velocity of 948 m/s at the centerline of the duct.

The laser depicted in Figure 3 is a Coherent model Innova 90-5 argon ion laser with green light of wavelength 514.5 nm. The laser and most of the transmitting optics were kept inside a mobile laboratory (see Figure 9). Incident laser beams were transmitted to the test site using two 30 m long optical fibers. The optics that were kept at the measurement site included the beam expander, focusing lens, and the receiving optics. The optical arrangement was done in such a way that the measurements were carried out in the forward scattering mode. The focusing lens was mounted on a remotely controlled traverse system in order to move the measurement point across the duct. The photomultiplier tube was kept near the signal processor inside the mobile laboratory. An optical fiber link was used to transmit the scattered signal from the receiving assembly to the photomultiplier. The signal processor used for analyzing the signal was a Doppler Signal Analyzer (DSA) designed by Aerometrics Inc.

The collection optics consisted of a 3.25" diameter lens of focal length 900 mm and a receiving assembly that focuses scattered light collected by the receiving lens onto the photodetector aperture. The alignment on the forward scattering side was maintained as the measurement volume is moved by means of a motion controller system from the mobile laboratory. This system consisted of two Newport 860A linear Motorizers which replaced the two thumb screw adjustments on the receiving assembly. These screw adjustments are used to focus the scattered light onto the photodetector. A 50 m long cable was used to connect the Motorizer with the

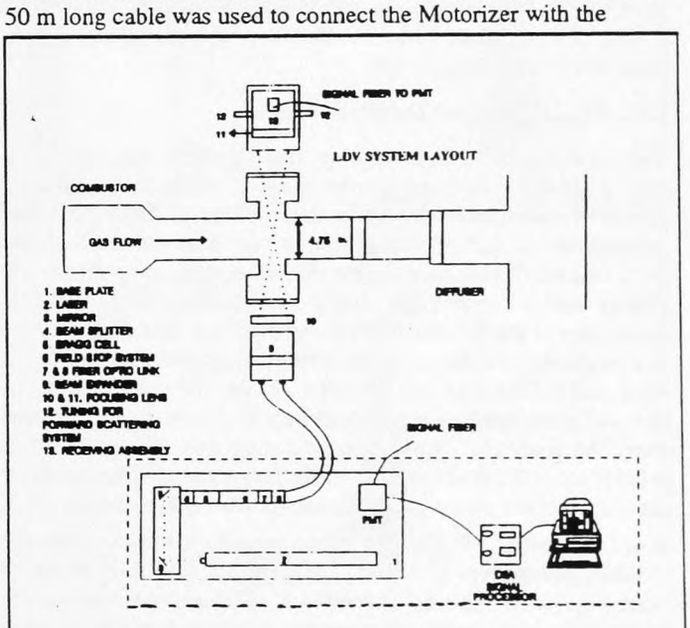

Figure 3. A Schematic Of The LDV Apparatus.

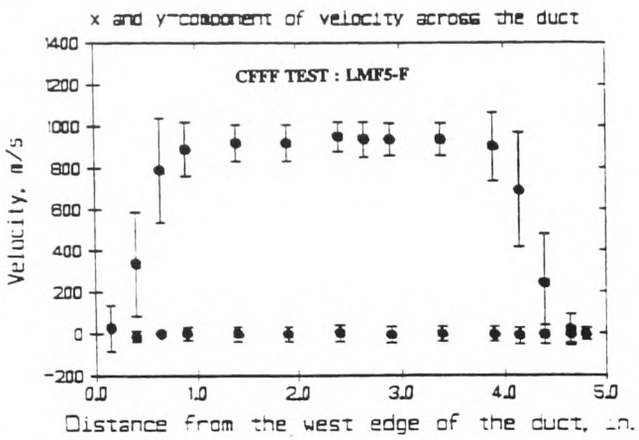

Figure 4. Axial (Upper) And Transverse (Lower) Velocity Profiles Across The Aerodynamic Duct.

hand-held motion controller. The Motorizer was adjusted with the motion controller by looking at the signal level on the oscilloscope and the intensity of the signal light on the Aerometrics Doppler signal analyzer. These adjustments are required each time the measurement volume is moved. Without this motorized system, it would not have been possible to maintain the alignment of the forward-scatter configuration, since access to the LDV equipment was very limited.

The accuracy in the measurement of velocity using a LDV system depends significantly on the value of fringe space (d_f). This is a calculated value and depends on the laser wavelength, beam spacer, expansion ratio, and the focal length of the lens. The focal length of the lens can be measured within $\pm$ 2 mm. The beam spacing and expansion ratio values are provided by the manufacturer and used as quoted.

The accuracy of the calculated value of the fringe spacing was tested by measuring the velocity of a wheel rotating at a known speed. The velocity of this rotating wheel is 16.6 m/s for the given r.p.m of 1800. The mean velocity value measured with the LDV setup used for this experiment was 16.4 m/s and is in good agreement with the calculated value. This suggests that using the calculated value of fringe spacing will provide a velocity value within 1 - 2% of the original value. At 1000 m/s, this represents a maximum uncertainty of $\pm$ 20 m/s

LDV RESULTS AND DISCUSSION

The combination of high velocity, small particle size, and reduction in the collection aperture to about 1" made the usual backscatter measurements virtually impossible. A forward scatter arrangement as described was used to overcome these difficulties. With this configuration we were able to measure the velocity profiles (x- and y- components) across the aerodynamic duct. A composite plot of the profiles is shown in Figure 4. The mean velocity (x-component) measured at the centerline position (2.4" from the west wall) of the duct was around 950 m/s. The velocity profile is almost flat except for the positions near both port openings. Moreover, the profile is symmetric indicating that the output of the combustor and upstream elements are symmetric. Measurements have been made previously at locations where the velocity profile is not symmetric.[3,12] Figure 5 shows a composite plot of the axial velocity component histograms at different positions across the duct. Figures 6-7 give an alternate and detailed presentation of the velocity (x-component) histograms at selected positions across the duct. It is interesting to note that the histograms display a bimodal character for positions near the wall and this disappears at about 0.9" into the duct. At positions closer to the wall of the duct, the low velocity part of the histogram becomes dominant. This phenomena was observed on both sides of the duct and is believed to be due to the presence of the optical ports. The y-component velocity profile is shown in the lower portion of Figure 4. The mean values were close to zero at every measurement position and displayed a range from about -100 m/s (down direction) to +100 m/s (up direction). Figure 8 shows a y-component velocity histogram at the centerline of the duct. The mean velocity value (y-component) was only 2.00 $\pm$ 37 m/s at this position.

It perhaps should be noted that each histogram represents about 1000 single particle measurements. Moreover, as a check of the performance of the signal processor, various Doppler bursts where digitally recorded and analyzed for the Doppler frequency. Velocities derived from this procedure were entirely consistent with the signal processor data analysis.

The effect of purge on the flow near the port walls was investigated by using a control system in which the port purge could be turned off for short times ($\approx$ 5 sec). The LDV measurements obtained during a "purge-off" condition showed no significant change from those during the normal "purge-on" condition. It was observed, however, that during the "purge-off" condition, slag particles accumulated at the window rather quickly. The purge which is typically used is within the range of 15-20 ft^3/min of nitrogen gas or argon gas. This is an extremely small amount compared with the combustion gas flow.

TEMPERATURE MEASUREMENTS

To measure the temperature at a point in the gas stream, a laser based technique was employed known as coherent anti-Stokes Raman spectroscopy (CARS). The measurements were taken at the same optical port where the LDV measurements were made.

The experimental CARS system and details of the method have been described elsewhere[5-7]. In Figure 9 we give a schematic illustration of the CARS measurement system. Briefly, the technique involves the use of two narrow band laser beams at pump frequency ω_1 and one broadband dye laser beam at Stokes frequency ω_2. The three beams are then phase-matched as depicted in Figure 10, and focussed by a lens to a point in the gas stream where the laser-like CARS signal is generated. The CARS signal occurs at the anti-Stokes frequency $\omega_3 = 2\omega_1 - \omega_2$ and is generated by a nonlinear process involving the third-order electric susceptibility $\chi^{(3)}$ of

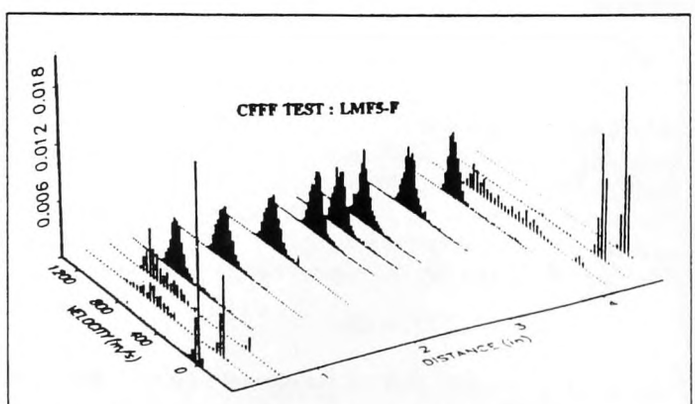

Figure 5. Composite Plot Of The Axial Velocity Histograms Across The Duct.

the medium. The intensity of the anti-Stokes signal beam is given by

$$I_{CARS} = \frac{16\pi^2 \omega_3^2}{c^4} \bullet I_{pump}^2 \bullet I_{Stokes} \bullet |\chi_{CARS}|^2 \bullet l^2 \qquad (6)$$

where the I's are the pump and Stokes laser beam intensities, l is the interaction length where the three beams overlap. Here it is assumed that the beams are properly arranged to insure that momentum conservation (phase matching) is fulfilled. The χ_{CARS} is the third-order susceptibility of the medium which consists of a frequency-dependent resonant part and a nonresonant part

$$\chi_{CARS} = \chi_{NR} + \chi_R(N, T, P, \cdots) \qquad (7)$$

where T is the gas temperature, P is the static pressure, and N is the probed molecule number density.

The use of a broadband dye laser permits the CARS spectrum of a species to be obtained with a single pulse of the laser. The center frequency of the dye laser is chosen such that $(\omega_1 - \omega_2)$ is close to a Raman resonance frequency of the species being measured. In the present case, for an air-fuel combustor, the nitrogen molecule is a major gas species and is hence used to extract the gas temperature. In particular, the shape of the N_2 CARS spectrum is sensitive to the gas temperature. To extract the gas temperature, the N_2-CARS spectrum is calculated for different temperatures and compared to the experimental spectrum.

As shown in Figure 9, the pulsed Nd-YAG laser and broadband dye laser are contained in the rear of an 18-wheeler type trailer. This mobile laboratory provides a means to transport and operate the CARS system. The trailer is parked close to the test facility. The pump and Stokes laser beams are sized, manipulated, and aligned as required for proper phase matching and to insure the three beams subsequently focus at their crossing point. The laser beams are sent out through a hole in the back of the trailer and directed to the test media using a series of right angle turning prisms. The two prisms are mounted on a rigid stand about 6 feet above the ground and the separation of the prisms may be changed to allow the laser beams to be aligned with the optical port. Traversing lenses at the port site are used to focus the laser beams into the test medium and collect the signal generated. The lens system consists of two converging lens. The first lens focuses the laser beams into the test region where the CARS signal is to be generated. The CARS signal, along with the original laser beams, are recollimated through the second traversing lens system and directed to the receiver. The lens are mounted on a translation stage

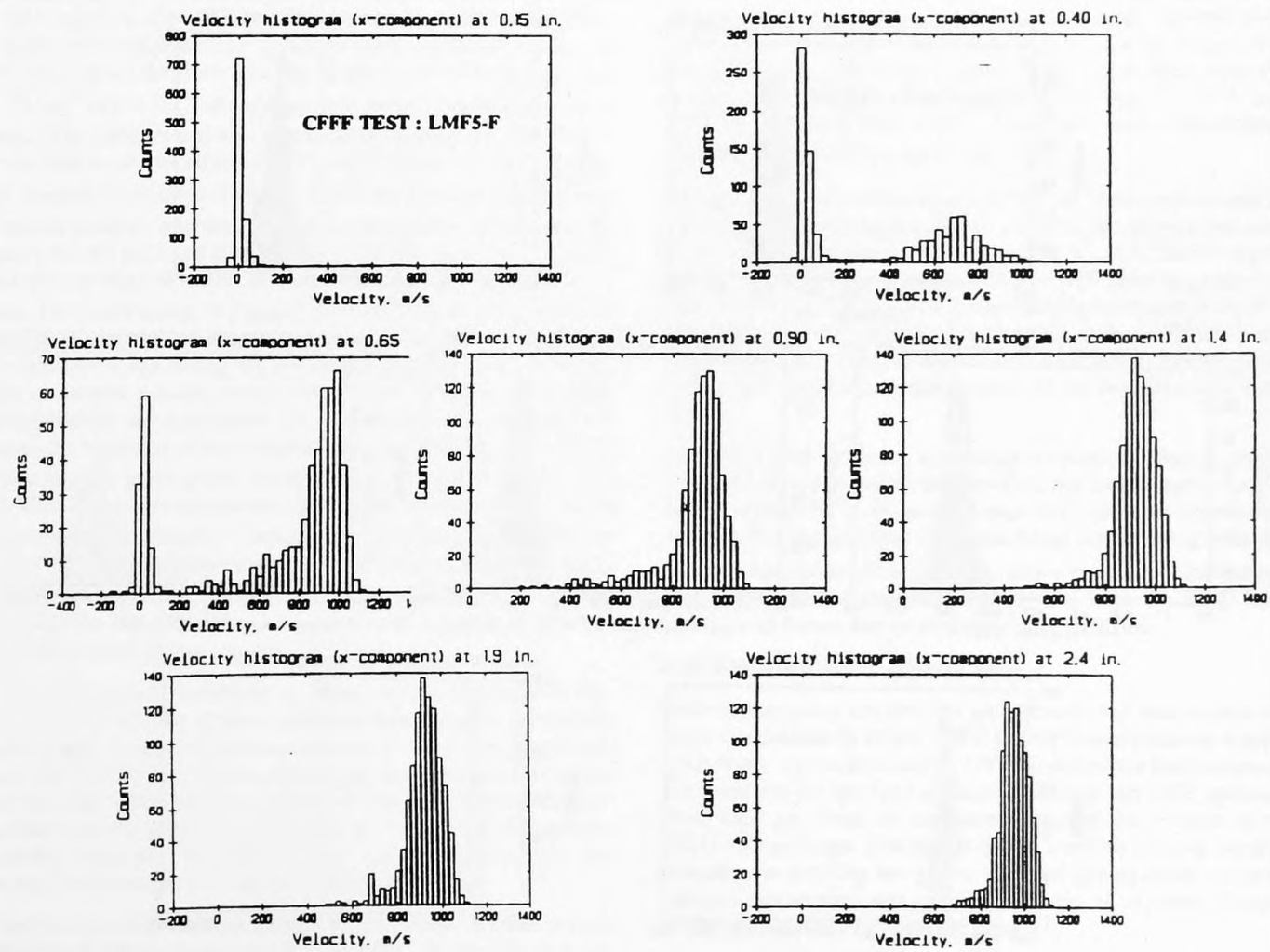

Figure 6. Detailed Velocity Histograms As One Moves From the West Wall Toward The Center Of The Gas Stream

and a computer-controller stepper motor is used to move the two lens together in the forward or backward direction. In this way, the focus point is moved across the gas stream allowing the temperature profile to be obtained.

The receiver contains a dichroic mirror and beam blocks which separate the CARS signal from the high intensity laser beams. The CARS signal is then coupled to an optical fiber with a suitable lens and a couple mounted on an x-y-z translator. The coupler may be remotely translated to maximize the CARS signal transferred to the optical fiber. The optical fiber brings the CARS signal to the spectrograph. The detector mounted on the exit of the spectrograph is a double intensified diode array (DIDA). The detected CARS signal and other important data are sent to a MICRO-VAX computer for analysis.

To reduce the large background from the high luminosity gas stream the DIDA detector was operated in a gated mode. An adjustable aperture was also mounted on the receiver table to further reduce the emission from the gas stream. By properly adjusting the gate pulse delay and pulse width with respect to the CARS signal, reasonable-quality CARS data could be obtained. A typical 200-ns gate pulse width and 100-ns delay between the rising edge of the pulse from the laser were used in the CFFF measurement. To improve the signal-to-noise, a series of spectra are averaged. In particular, the spectrum in Figure 11 represents the accumulated detector average of some 100 laser pulses (10-sec average). This spectrum, when analyzed, gives a time averaged temperature. A set of such CARS spectra (say 10 or so) are collected at each point across the gas stream. Each spectrum in a given set is analyzed for the temperature. The average temperature is then computed for the data set along with the standard deviation. This procedure provides the temperatures and deviations shown in the following figures.

CARS RESULTS AND DISCUSSION

The mobile CARS system was aligned at the CFFF aerodynamic duct during the October LMF5-G test run to measure the temperature profile. The aerodynamic duct CARS data showed interference from laser-induced breakdown (LIB) effects. This breakdown occurs because of the high laser power needed in these measurements and this breakdown generates atomic emission lines which can interfere with the CARS signal. Figure 12 shows a typical laser induced breakdown emission spectrum. Some of the atomic emissions are identified in the figure. This spectrum is obtained by blocking the Stokes beam so as not to generate a CARS spectrum. Also shown in the figure is a CARS spectrum with accompanying breakdown emission. Though careful alignment could reduce this emission it is doubtful that its effects can

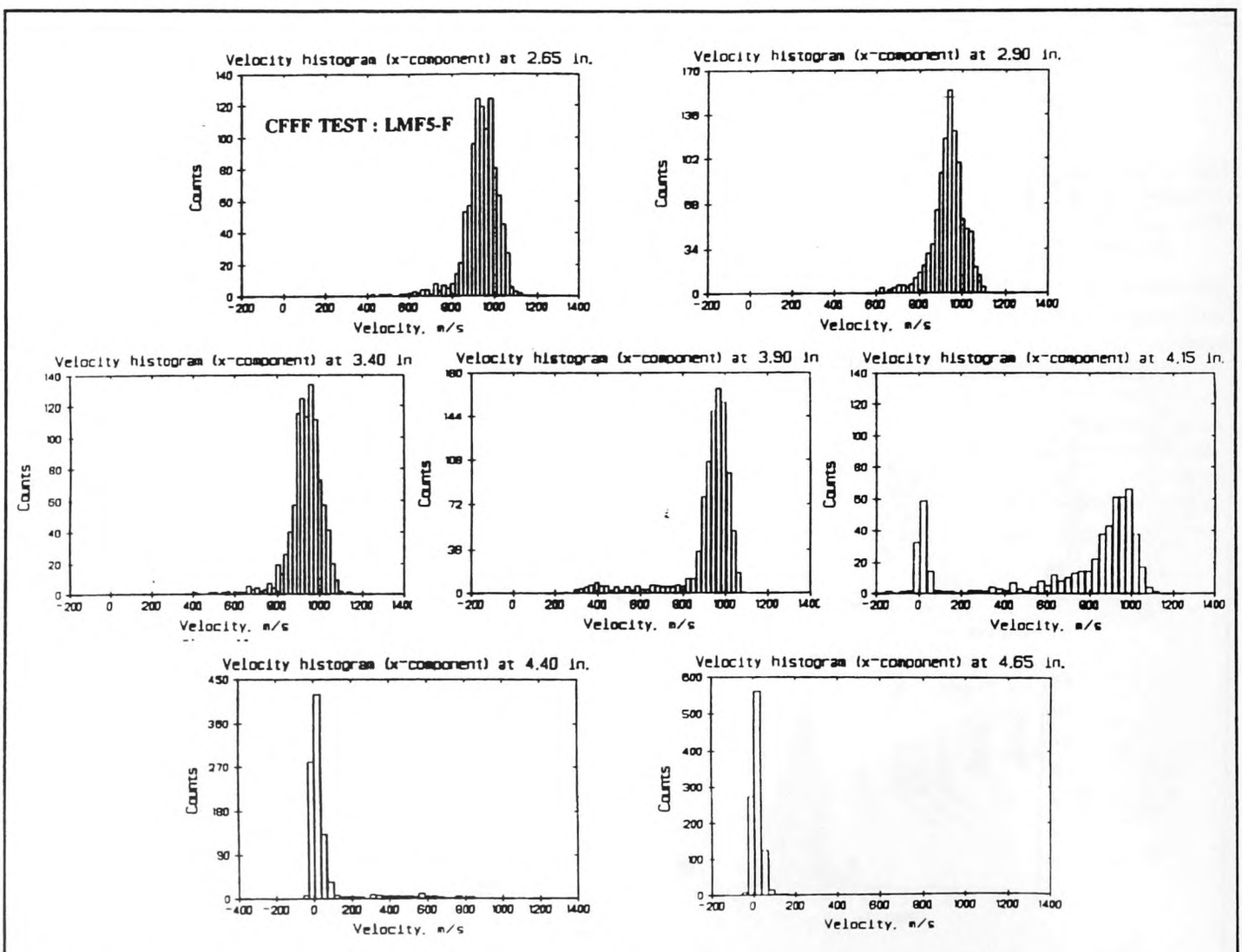

Figure 7. Detailed Velocity Histograms Moving From The Central Gas Stream Region To The East Wall Of The Duct.

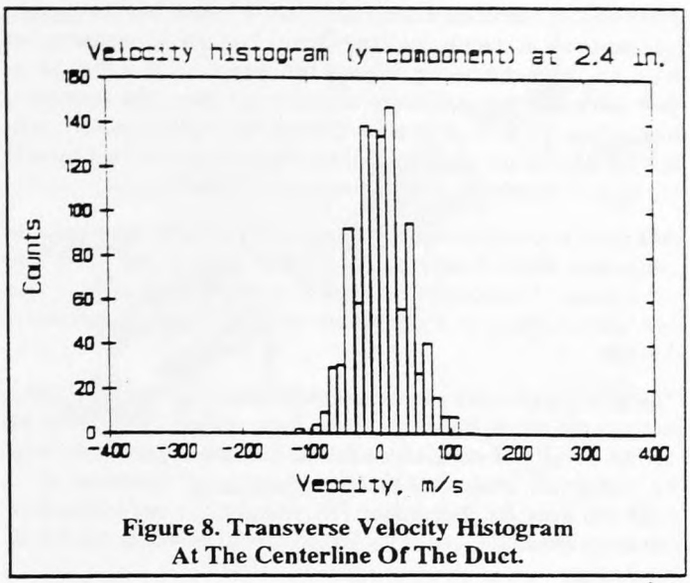

Figure 8. Transverse Velocity Histogram At The Centerline Of The Duct.

be completely removed. Note strong emission lines overlap with parts of the N_2 CARS spectrum. In addition, there is a large nonresonant contribution due to particle induced breakdown[13]. This nonresonant particle effect was found to be larger in the duct (particle density higher) than that found in the diffuser. This gives the gaussian-shaped spectrum shown in Figure 12 upon which the CARS spectrum appears. Figure 11 shows a typical CARS spectra (upper curve) taken at 0.25" from the center of the gas stream on the east side of the duct. The dip in the observed spectrum near 2320 cm^{-1} is due to C_2 absorption and occurs at the 0-1 N_2 CARS band. The temperature was extracted by fitting the spectral regions which are not effected by C_2 absorption. This complicates the analysis since most of the 0-1 N_2 CARS band must be omitted from the analysis, and the temperature determination depends primarily on the hot-band data. Usually, one fits both the cold band and the hot band of the N_2 CARS spectra to extract the temperature. The lower curve of Figure 11 is the difference between the calculated and observed spectrum. Moreover, because of the substoichiometric conditions, the concentrations of various hydrocarbon molecular species, which contributed to the nonresonance susceptibility, are not known very accurately. To take into account the variation of the nonresonant susceptibility and the N_2 concentration in the probe volume, the C parameter (ratio of the N_2 mole fraction to nonresonant susceptibility) was floated in the least squares fit. Figure 13 shows the temperature profile near the center of the gas stream extracted from the N_2 CARS data taken at different times during the test run of October 1992. The inferred temperature was essentially a constant over a length of about 2" near the core of the gas stream.

The large standard deviations ($\pm$ 200K), which are found in Figure 13, arise because of the significant turbulence of the rapidly moving gas stream and the time response of the measurement system. To obtain, e.g., reasonable signal-to-noise, time-averaged spectra were collected over a period of about 10 second and during this time the gas stream moves about 10,000 m and its instantaneous character fluctuates many times. Nonetheless, the average temperature can still be quite meaningful.

However, the additional complications mentioned previously can affect the derived temperature. For example, the temperature obtained by fitting mainly the hot band and a small part of the cold band can be high[14] by as much as 100 K. Also any contribution to the measured spectra from breakdown emission in the hot band region can lead to a higher derived temperature. The slight differences in the fit of an observed spectrum at two temperatures differing by 200K is shown in Figure 14. These considerations lead one to expect that the derived CARS temperatures are most likely high in the central core region of the flow.

As one moves toward the wall, the CARS temperature decreases on both the east and west sides of the gas stream. Analysis of the CARS data closer to the walls shows that there is a mixing of cold and hot temperature spectra in the measurement volume. Because of the limited optical access, the measurement volume was between 1 and 2 cm long. To prevent cold N_2 from entering the gas stream during these measurement, the optical ports were purged with argon. However, near the walls, the purge tends to cool the gas (N_2) and the effect of the purge and turbulence gives CARS spectra near the boundaries which are mixtures of cold and hot N_2 spectra. It has been noted previously, that the fitting of a bi-model temperature spectrum will only extract a volume averaged temperature[15]. This is why the temperature profiles extracted from the time averaged CARS data show a significant temperature drop starting from 1" away from the gas stream center. This leads to a much wider boundary layer than is actually present in the flow.

MODELING AND RESULTS

Discussions of data analyses and numerical model simulations of the flow field within the CFFF LMF supersonic aerodynamic duct are provided in following material. These simulations were undertaken as part of an overall collaborative study by MSU and UTSI to institute MSU's optical access techniques and systems (OATS) in the CFFF upstream test train.[9]

As part of this cooperative effort, UTSI was consigned the task of providing their assessments of the experimental plasma measurements that were taken by MSU-DIAL using their OATS during the 1992 LMF5 tests series. MSU provided these experimental data to UTSI - UTSI, in turn, independently evaluated these data based upon their familiarity with operation of the CFFF LMF system and by performing independent numerical simulations of the CFFF LMF upstream plasmadynamics to use in comparison to the data.

The UTSI data analyses and plasmadynamic modeling results provide a means by which the flowfield and heat transfer that develops within the LMF aerodynamic duct could be confidently viewed. The independent UTSI modeling results along with numerical simulations of MSU[4,7,16] form a basis by which the experimental velocity and temperature data from the MSU laser plasma diagnostics can be compared and qualified.

THERMODYNAMIC ANALYSES

Prior to attempting any detailed gas dynamic and heat transfer numerical calculations of the CFFF LMF plasmadynamics, a more basic study was undertaken by UTSI to define the thermodynamics processes for the flow expansion through the LMF upstream flow train, i.e., from the combustor through the location of the MSU optical flange. The results of this exercise prove to be most revealing in defining the global range of gas dynamic variables (plasma temperature and velocity) that can be expected. Results of these studies are provided in Figure 15.

The NASA SP-273 thermochemical equilibrium computer code[17] was used to construct the plots presented in Figure 15. This code

computes the ideal coal combustion process (combustion to thermochemical equilibrium) to define the combustion gas constituents and its thermo- and gas dynamic transport properties. The NASA SP-273 code was subsequently run in its _rocket mode", wherein, calculations were made for an isentropic expansion process.

The expansion process calculations were initiated from a defined combustor stagnation state. Perturbations on the combustion stagnation state were impressed by specifying the combustion chamber pressure at a level nominal for western coal POC operation (4.51 Atm) and then imposing variable levels of heat loss. This type of parametric calculation provides a definition of the thermodynamic state points through a supersonic flow expansion of a real gas (in this case, coal combustion products).

It was sought in this study to arrive at "bounding" levels of the temperature, velocity, and plasma conductivity at various locations along the CFFF LMF upstream test train.

These "bounding" levels could in turn be used to define limits on the thermodynamic variables within which MSU plasma measurements should be contained. The locations of interest are the combustion chamber, the nozzle throat, the nozzle outlet, and the location of the MSU optical flange. Each of these locations were specified in the calculations by definition of the expansion ratio (A/A*). The various lines shown on the plots of Figure 15 represent these specific locations.

The ideal flame state for the CFFF LMF test train with burning of western coal at the operating point of Table I is defined in Figure 15 by the solid line representing the combustor. Subject to adiabatic, complete combustion, the ideal flame state is predicted at a temperature of 2872K with conductivity at 11.2 S/m. Of course in the real situation, where heat losses reduce the thermal state of combustion (stagnation state of the flow expansion), the flame condition is substantially reduced.

The shaded regions shown on the plots of Figure 15 identify an estimate of the range of heat loss that is normally experienced in operation of the CFFF LMF with western coal. The span of this shaded region across the heat loss scale illustrates variation in heat transfer that is seen to occur in LMF5 testing. This variation is a consequence of variations in the coal slag coverage that occurs with run time.

Furthermore, the shaded areas of Figure 15 represent the cumulative heat loss as the plasma flow moves through the upstream test train, i.e., from combustor, through the nozzle and then through the first section of the supersonic aerodynamic duct. The increase in heat loss as the flow progresses through this region can be seen by tracing through the mean level of the shaded region across the plotted lines in the direction from combustor to MSU flange.

At a mean level of heat loss as experienced in LMF5, the flame state (stagnation state) is substantially reduced from the adiabatic state cited above. A reasonable estimate of the flame state during actual operation would be at a temperature of 2725K and conductivity of 5.9 S/m.

The axial location of most interest in this study was the MSU flange location (shown in Figure 15 by the large dashed line). Reviewing the NASA SP-273 calculations for this location as given here, it can be confidently contended that for _supersonic" operation of the LMF test train; the temperature (**T**), velocity (**U**), and conductivity (σ) measurements taken at the flange should be within the following bounds:

$$2545K > \mathbf{T} > 2315K$$
$$1342\ m/s > \mathbf{U} > 1290\ m/s$$
$$6.2\ S/m > \sigma > 2.0\ S/m$$

These bounds are considered extreme broad—they extend from an ideal adiabatic flow situation through a heat loss level above that experienced in any LMF5 test.

From a review of the experimental data that are presented in the previous and later sections of this paper, it is apparent that the MSU plasma measurements are well outside of these bounds. The CARS temperature profiles indicate plasma temperature at centerline points in the measurement cross-section above those limits given above. Similarly, the LDV measurements of velocity profile show a mean velocity level across the flow core region in the 900 to 1000 m/s range which is well below these limits.

The discrepancy between the MSU OATS measurements and the results of this theoretical study provided a first indication in these data analyses efforts that::

The Flow At The MSU Optical Flange Is Subsonic.

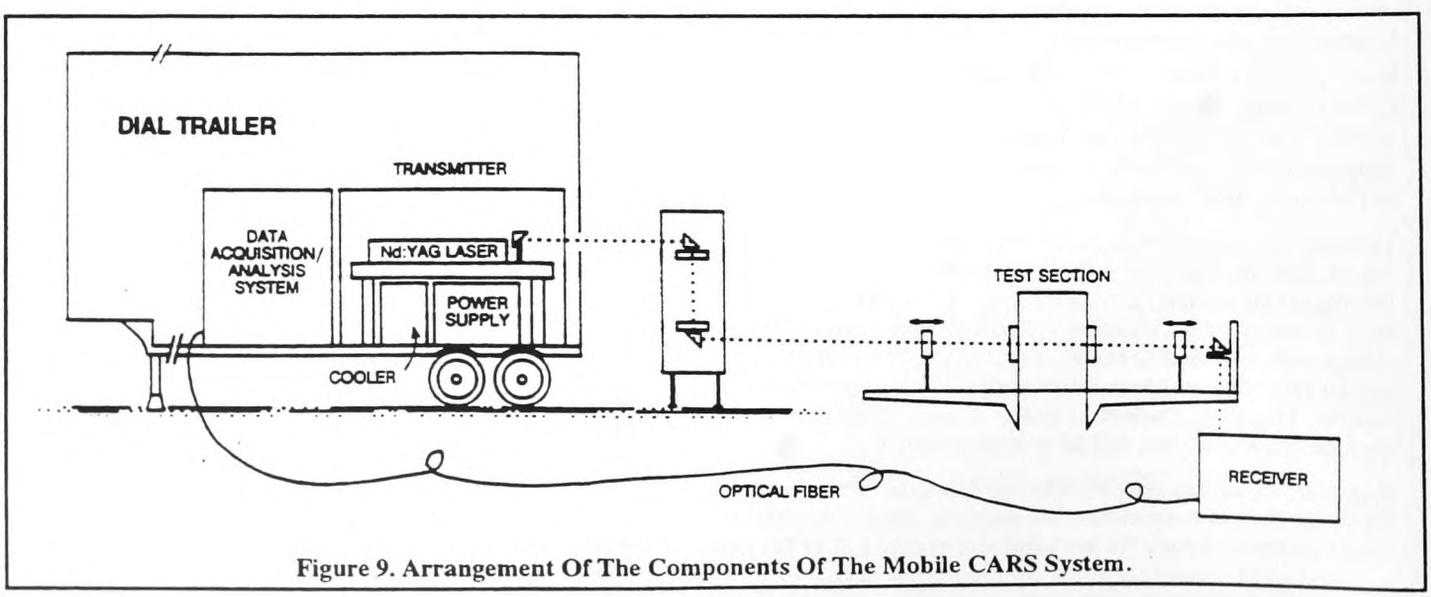

Figure 9. Arrangement Of The Components Of The Mobile CARS System.

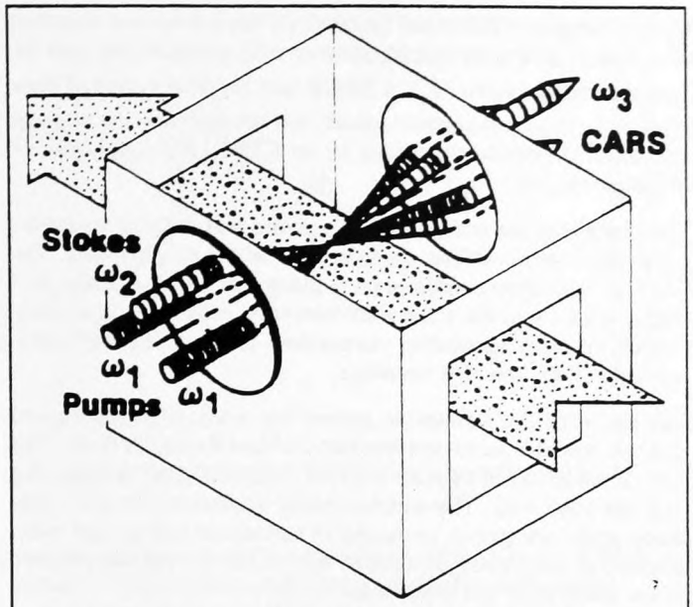

Figure 10. Laser Beam Configuration For Folded BOXCARS Phase Matching.

The measured temperatures and velocities that were extracted using MSU's OATS laser diagnostics are more representative of those levels indicated by the calculation in Figure 15 for the nozzle throat station. That is, at the sonic point, static temperature around 2550K and flow velocity around 910 m/s were measured. From this observation, it has been hypothesized by the MSU-UTSI researchers that:

"the presence of the MSU optical flange at the exit of the CFFF LMF aerodynamic duct (section 1) provides a flow restriction of such a magnitude that the flowfield in the duct upstream of the flange is driven subsonic. The action being observed is a shift in the location of the flowfield choke point from the geometric nozzle throat to the location of the Optical Flange."

The possibility that this type of action could occur was first speculated upon by UTSI in the early stages of this collaborative research - when the Optical Flange was designed and installed in the LMF test train. Moreover, it was noted then that the slight loft discontinuity due to the flange installation between first two aerodynamic duct sections, in conjunction with, the requirement for mass injection at the flange (a continuous N_2 purge supply to the optical port window to maintain visibility) - presented a situation wherein a shift in the choke point of the flow was a possibility. This shift being brought about by the combined actions of loft compression at the flange, mass injection at the flange, plus, enhanced frictional (Fanno) and heat transfer (Rayleigh) effects.

UTSI FLOW FIELD SIMULATIONS

Multidimensional modeling of the CFFF LMF gas dynamics and heat transfer through the first section of the aerodynamic duct was concluded by UTSI as part of this collaborative research. These studies addressed design point operation of the LMF upstream test train which is simulation of its normal supersonic operation.

The objective of these flow field studies was to provide simulations which could be used in comparison to the MSU experimental data. The modeling was directed at producing predictions of the gas dynamics and thermodynamic properties of the flow as would exist at the entrance location of the MSU Optical Access Port for design operation of the LMF test train at western coal POC conditions. In addition, the multidimensional modeling approach was selected to produce theoretical profile shapes of these variables which could be compared to the measured spatial distributions of the MSU experimental data.

MODELING METHOD

The principal numerical technique used in the UTSI modeling was the VNAP2 computer code.[18] This code is widely recognized in the computational fluid dynamics (CFD) field. It has been modified for use at UTSI in the past to address a variety of internal flow problems, including, flow field transients, nozzle and duct design problems, and (with considerable work to incorporate MHD terms and processes) MHD generator studies and MHD transients.[19]

VNAP2 is a user oriented computer code that can be used in the design and analysis of complex internal flows. It was set up in this work to tailor it for application to the high Reynolds number, high temperature coal combustion gas flow of the CFFF LMF upstream test train.

The VNAP2 solution technique solves in axisymmetric coordinates the two dimensional, time-dependent, Navier-Stokes and energy equations. Turbulence can be modeled with either a mixing-length, a one transport equation, or a two transport equation model.

Features of the VNAP2 numerical scheme that are used to solve the governing finite difference equations include a nonequal-spaced grid system with transformation of the physical geometry into a rectangular computational plane.

Interior grid points are computed using the explicit MacCormack scheme with special procedures implemented to speed up the calculation in the fine grid.

VNAP2 can address internal or external flows through definition of boundary values. For internal flows, subsonic or supersonic flow across the inflow and outflow boundary can be imposed which facilitates calculations through a supersonic nozzle or a separated flowfield. VNAP2 employs an explicit artificial viscosity to stabilize calculations. The code is capable of treating

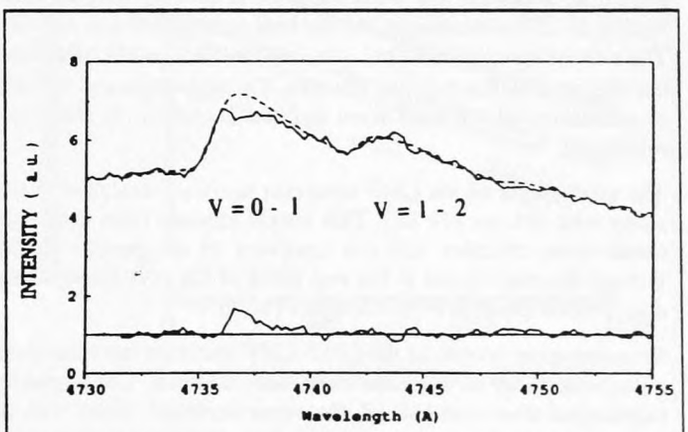

Figure 11. CARS Spectrum Recorded At The Aerodynamic Duct During The LMF5-G Test Run. P = 0.25", T_{fit} = 2556 K. The Lower Curve Is The Difference Between The Calculated And Observed Spectrum.

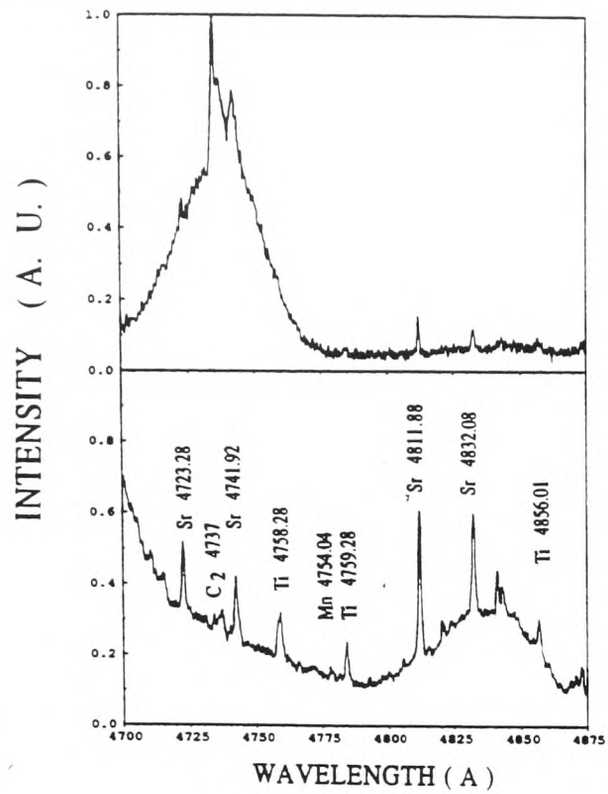

Figure 12. Upper Curve Shows A CARS Spectrum With Laser Induced Breakdown Emission. The Lower Curve Shows A Laser-Induced Breakdown Spectrum Obtained By Blocking The Stokes Beam. Some Of The Atomic Emissions Are Identified In The Figure.

through mixed flow regimes (across the sonic point), separated flows and flow across jump conditions (e.g., shock waves).

For more detail and background on the VNAP2 computer code and its modeling methods, referral is made to the references 18 and 19 of the bibliography

COMPUTATIONAL SET-UP

For the calculations presented herein, the combustion gas was treated as a perfect gas with transport properties defined from NASA SP-273 calculations for the coal combustion gas mixture. The ratio of specific heats (γ), gas constant (R), and Prandtl number (Pr) were defined for the mixture. The stagnation and the static conditions at the inlet were defined according to isentropic relations.

The total length of the LMF upstream test train analyzed in this study was 104 cm (41 in.). This length extends from inside the combustion chamber (23 cm upstream of the nozzle throat) through the nozzle and to the exit plane of the first aerodynamic duct section (inlet to MSU Optical Flange).

Since the cross section of the CFFF LMF upstream test train is circular, symmetry of the flow field was assumed. Consequently, calculation over one-half of the cross-sectional plane was required in modeling with symmetry defined along the centerline. The non-uniform mesh configuration that was used consisted of 81 x 41 grid nodes in the axial and radial directions, respectively.

In-flow boundary condition imposed on the calculation was that of subsonic flow with specification of total pressure (P_o) of 4.51 atm, total temperature (T_o) of 2800K and the distribution of flow direction. These stagnation values are consistent with western coal POC stagnation conditions in the CFFF LMF combustor as noted previously.

The outflow of the computational volume was defined for supersonic flow with outflow boundary variables extrapolated. The "no-slip" boundary condition on velocity was imposed along duct walls. In addition, the walls were treated as constant temperature (1800K) thereby simulating temperature and heat transfer representative of molten slag coverage.

The two-equation turbulence model was used. (It is recognized that this model is more representative of low Reynolds flow.) The turbulence model defines a very fine computational node spacing near the solid wall. The wall boundary conditions for the turbulence model are that of vanishing of turbulence energy and specification of turbulence dissipation rate so that the normal gradient of the dissipation rate is set equal to zero.

The pressure is actively calculated using the code's basic method of characteristic solution technique. The pressure prediction is recovered and corrected upon completion of each full iteration by recomputing it from the equation of state. During the calculations of each time step, the thermodynamic and molecular transport properties that are required in definition of viscous effects and the real gas equation of state are updated. These updates are derived from the use of curve fits of NASA SP-273 thermochemical equilibrium calculations for coal combustion gas.

MODELING RESULTS

The results of the VNAP2 calculations for supersonic operation of the CFFF LMF upstream are provided in Figures 16 through 18. These results show flow distributions typical to compressible, supersonic flow through an axisymmetric duct.

Figure 16 presents the computed Mach number contours. These contours define the flow field as it accelerates from the near stagnate conditions of the combustor, through the nozzle (passing subsonic to supersonic through the nozzle throat sonic point), and through the LMF aerodynamic duct. The sonic line is defined near

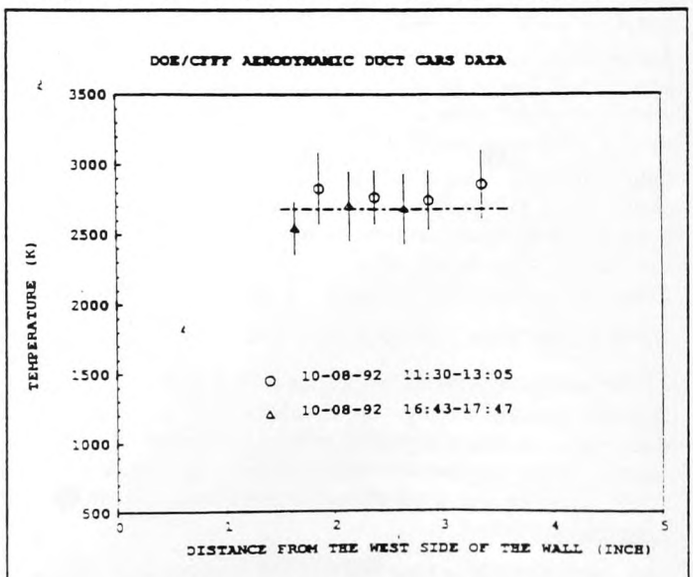

Figure 13. CARS Temperature Measurements In The Central Region Of The Gas Stream.

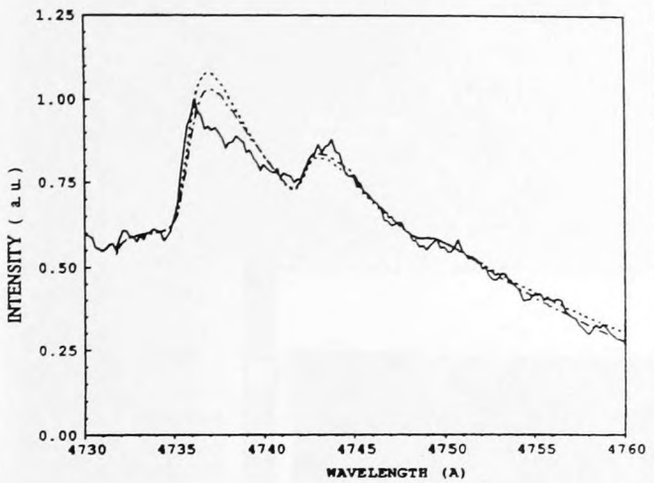

Figure 14. An Observed Cars Spectrum (Solid Curve) Which Gives A Temperature Of 2700 K With The Calculated Spectrum (Large Dashed Curve). Included Is The Calculated Spectrum At 2500 K.

the nozzle minimum area (throat) and depicts flow choking situation at design point operation.

Both the Mach number and pressure contours (Figure 17) exhibit flat profiles across the core region of duct. Very thin boundary layers form over the duct walls. From this point-of-view, the flow is nearly one-dimensional over this length of the LMF aerodynamic duct.

Some distortion in the contour plots is noticeable toward the exit plane. This distortion shows up as a bulge near the centerline in the downstream pressure contour and a similar, but lessnoticeable, bump in the Mach number exit contours. This distortion is not considered real. It represents the influence of the imposed out flow boundary condition and the impressed centerline symmetry.

DATA COMPARISONS

Comparisons between the VNAP2 flow field modeling and the MSU-DIAL experimental data are given in Figures 18. It is noted that the data studies of the previous subsection along with review of the MSU experimental data provided evidence that the flow within the Optical Flange was subsonic. Consequently, the VNAP2 calculations which were performed for design operation of the LMF upstream (supersonic flow) can be expected to provide only additional insight to help explain the measured profiles. The supersonic calculations are presented here to report on the complete study of this research effort and they also provide a first publication on multidimensional model simulation of the LMF upstream aerodynamic duct..

Figure 18 gives a plot of the VNAP2 predicted velocity profile across the exit plane of the supersonic aerodynamic duct. These computations are compared to the MSU LDV velocity profile measurements taken with the OATS at this location.

The shape of the predicted supersonic velocity profile is representative of the high Reynolds, highly turbulent flow. That is, the profile shape is flat over the core region and exhibits a thin boundary layer along the duct walls. The experimental LDV data also exhibits a very flat, turbulent type velocity profile shape across the core of the flow field. At the same time, these data exhibit the effect of the disturbance of the flow near the optical port. The

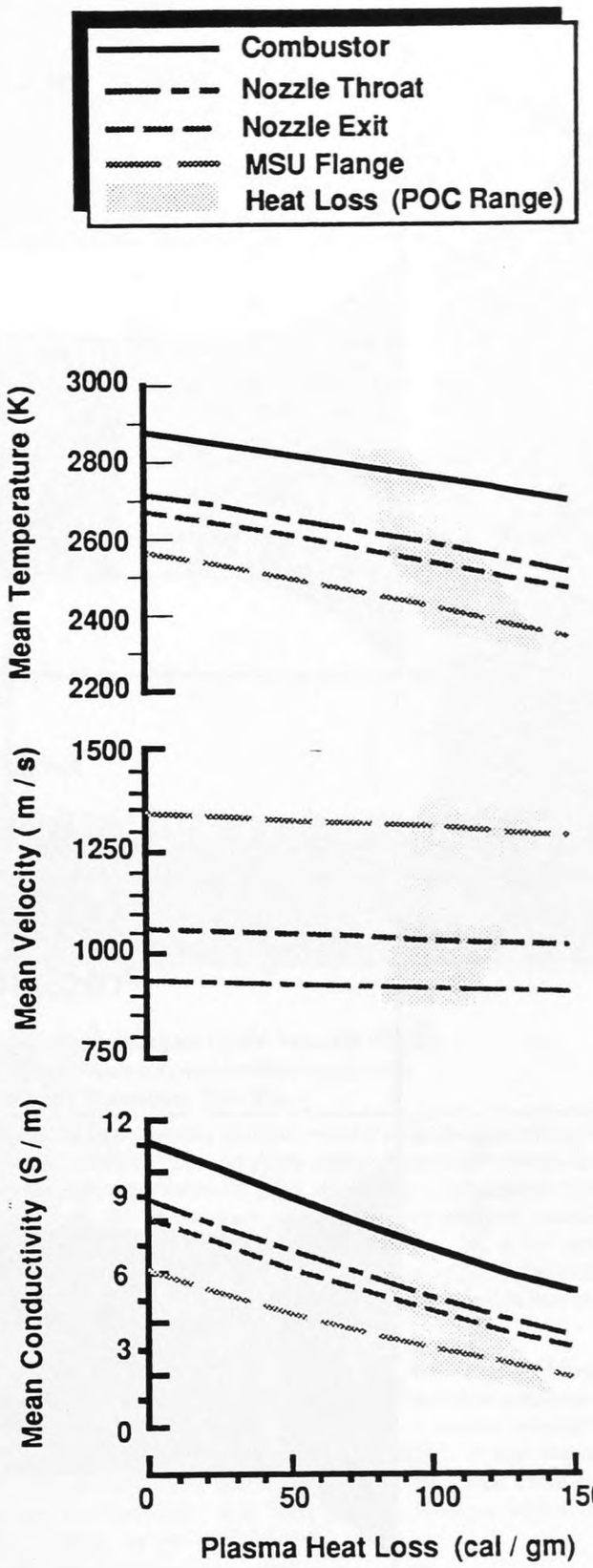

Figure 15. Ideal Thermodynamic Expansion Process for CFFF LMF Western Coal POC Operation— Results of NASA SP-273 Calculations.

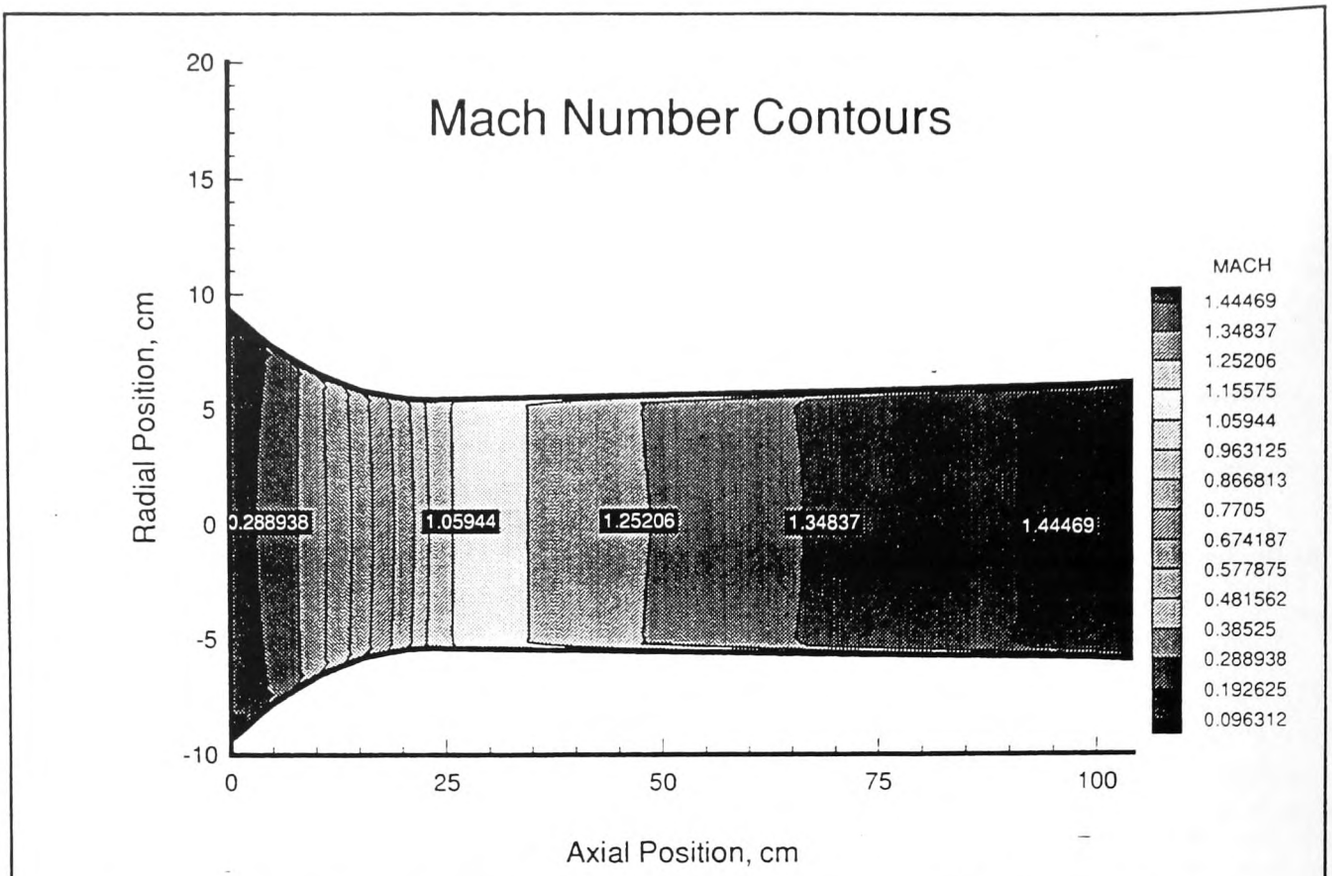

Figure 16. Simulations of the CFFF LMF Upstream Test Train Flowfield—Mach Number Contours

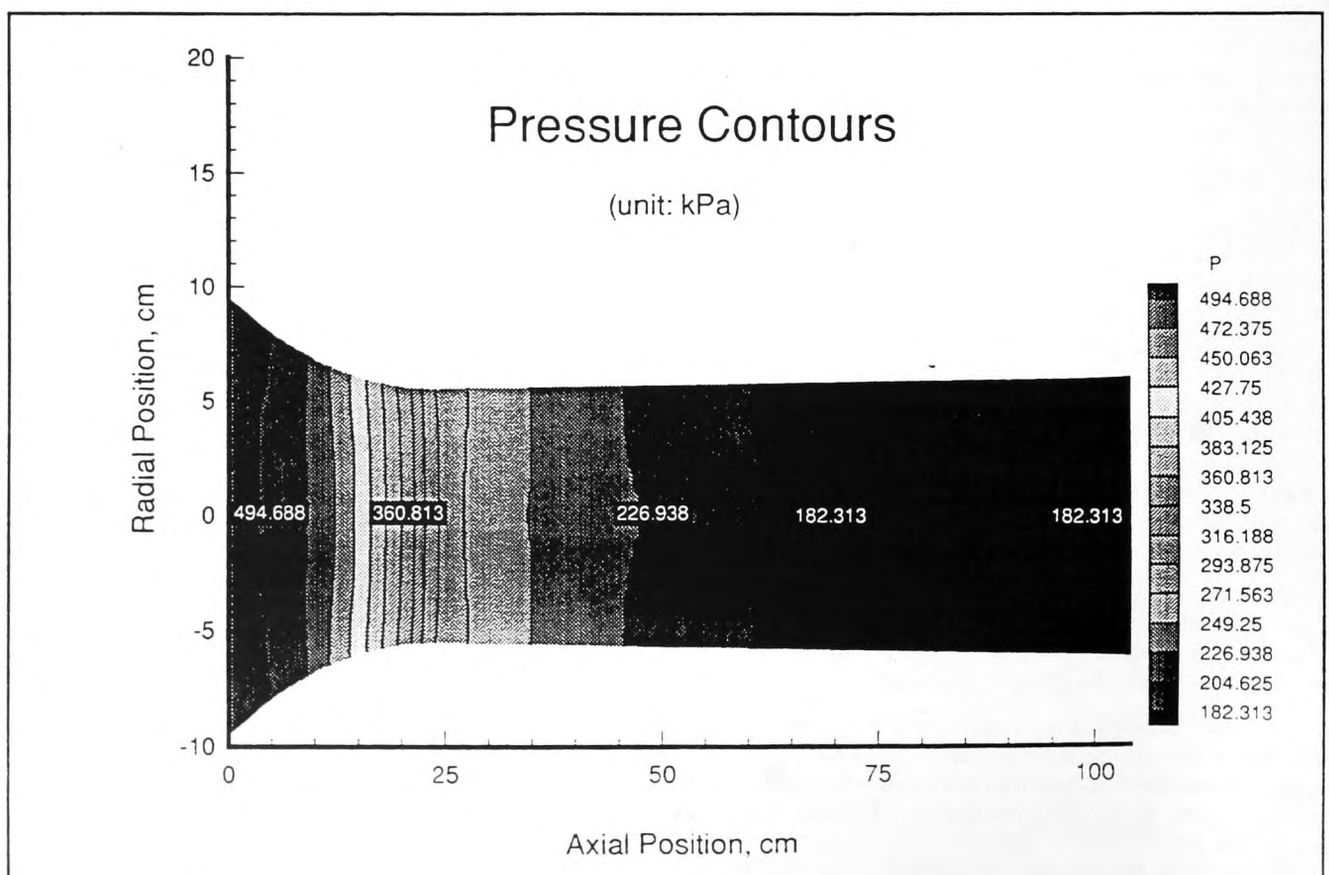

Figure 17. Simulations of the CFFF LMF Upstream Test Train Flowfield—Static Pressure Contours

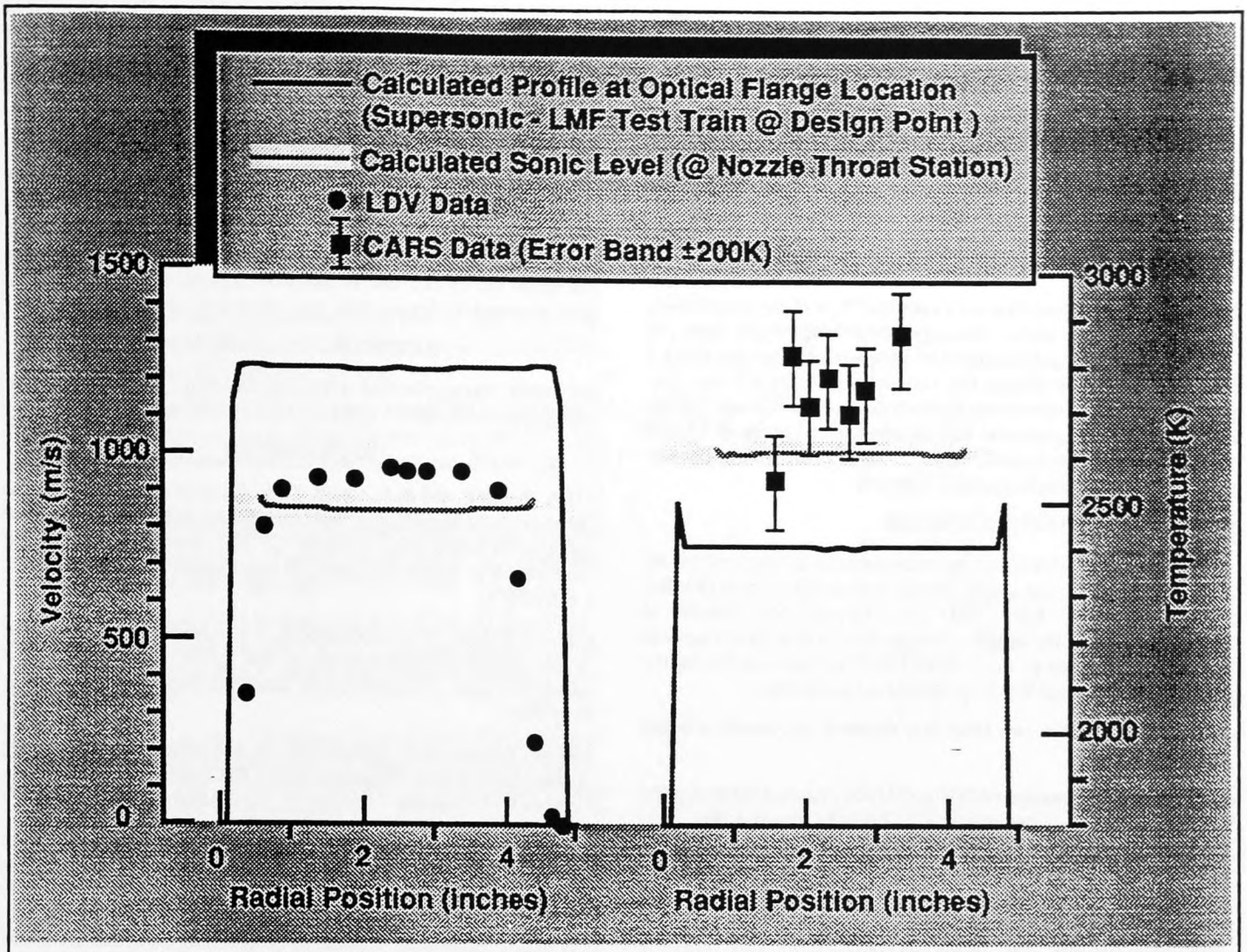

Figure 18. Comparison Between MSU OATS Plasma Measurements (LDV Velocity Profile and CARS Temperature Profile) to UTSI Computed Plasmadynamics for Supersonic (Design Point) Operation of the CFFF LMF Upstream Test Train

measured velocity distribution decays rapidly on both sides of the duct within about 2.54 cm (1.0 inch) of the cylindrical wall. This decay is a manifestation of the optical flange, i.e., a local flow disturbance caused by the loft discontinuity (wall penetration) at the port location.

The supersonic computed velocity profile is predicted at a much higher velocity level than the experimental data implies. The computed velocity is well above that measured with the LDV for all spatially distributed points. The level of core velocity at the nozzle throat as taken from the computed results is also provided in Figure 4 for reference. It is noted that this level is more consistent with the LDV measurements.

The comparative observations of the computed velocity to LDV measurements arrived at above is indication that subsonic flow actually exists through the upstream test train (from combustor to the flange location) during actual LMF5 testing. This hypothesis is in direct agreement with the findings cited previously. The near agreement between sonic velocity level and LDV measured velocity level leads to the contention that the actual velocity in the flange at the measurement location is very near sonic.

Figure 18 also provides comparisons between the supersonic temperature profile at the end of the aerodynamic duct section to the temperature data obtained using the CARS at the optical flange. Here again, the temperature calculations give classical renditions of supersonic, compressible turbulent flow; e.g., a flat profile across the core—a temperature rise near the wall to adiabatic recovery—a rapid fall-off to the wall temperature value across the near wall thermal boundary layer.

The temperature data given in Figure 18 were selected from the full spatially distributed CARS data set. These data points are the central most measurements. The large error bounds specified by MSU for these data are included (± 200K). Within the error bounds, the data infer that a flat temperature profile shape exists across the core. The mean level of temperature as indicated by these data is around 2700K ±200K.

The level of temperature consistent with the sonic line that was computed across the core of the flow at the nozzle throat is shown in Figure 18 for comparison. This level (approximately 2600K) is closer in agreement to the CARS temperature measurements. However, even the sonic static temperature core level is some-

what lower. In reality one would anticipate that this would be higher since it is subject to less heat loss.

The higher mean level of temperature that was measured by the CARS when compared to the supersonic flow calculations imply the actual existence of a lower speed flow in the LMF duct. Consequently, the same conclusion can be roughly drawn from temperature evaluations as was drawn for the velocity evaluations. That is, these temperature data suggest that the actual flow field through the flange was subsonic rather than supersonic.

It should be pointed out that for a subsonic flow at the optical port, the pressure will be higher than expected for supersonic flow. All of the CARS data analysis reported here were carried out using a library of computed spectra for a static pressure of 1.5 atm. (expected for a supersonic flow). Preliminary results indicate that the derived CARS temperatures will decrease in the range of 50-100 K as the pressure increases from 2-2.5 atm. Further analysis is underway and will be subsequently reported.

SUMMARY AND CONCLUSIONS

The work reported in this paper summarizes the most recent results of a collaborative experimental and analytical research between MSU-DIAL and UTSI. This research was directed at demonstrating the capability of extracting on-line measurements of plasma properties in a coal-fired MHD system—in the regime of the highly stressed MHD generator environment.

Major conclusions drawn from this research are provided in the following briefs.

•It is believed by between MSU and UTSI research team that the experimental data taken with the CFFF LMF Optical Access System (OATS) are good. The LDV velocity data that was taken are considered to be exceptional; providing a clear, concise view of a turbulent velocity profile across the circular duct as one would anticipate. Similarly, the CARS temperature data are also reasonably good within the larger uncertainty of this type of measurement in the environment of the duct.

• In order to improve the measurements by the CARS technique in the aerodynamic duct, it is necessary to reduce the interference effects, i.e., breakdown emission, and C_2 absorption. To avoid these interferences the pump and Stokes laser frequency need to be carefully selected to generate the N_2 CARS in a spectral region that is free from those laser induced transitions. This can be accomplished by selected an alternate pump laser e.g., an excimer laser.

• One key result drawn from this collaborative research (through its data interpretation, the modeling efforts, and through hands-on experimentation) is the indication that subsonic flow exists through the first aerodynamic duct section of the LMF CFFF upstream due to the influence of the Optical Access Port. The levels of temperature and velocity measured at the port are strong indications that the flow field is choked at this location.

• The multidimensional modeling used in this research represents the first such calculation that has been attempted at UTSI to simulate the mixed flowfield of the upstream CFFF LMF test train. This calculation extended along the length of the test train from near stagnation conditions within the combustion chamber, through the supersonic nozzle, and through the first section of the LMF aerodynamic duct.

• Finally, it is recognized by the authors and their respective organizations that the collaborative research between MSU and UTSI has been a resounding success. This research set out in 1992 to demonstrate to the scientific community that on-line optical measurements of an MHD coal-combustion plasma could be made in the highly stressed, thermodynamic environment that is typical to that existing in the coal-fired MHD generator.

The results presented in this paper and other recent publications on this research effort exemplify that this objective has been met; and, that optical diagnostics for coal-fired MHD are near being a state-of-the-art technology. What remains to be done is to refine and adapt the OATS and its laser techniques to the MHD coal-fired power plant for monitor and control of plant processes.

ACKNOWLEDGEMENTS

This work was performed with support from DOE Contract No. DE-AC02-80ET-15601 and DE-AC02-79ET-10815.

REFERENCES

1.R.A. Kumar, and R.L. Cook, "The Role of Advanced Optical Diagnostics in Monitoring and Controlling an MHD Power Plant part II - 50 MWt POC Topping Cycle." Eleventh International Conference on MHD Electrical Power Generation, Beijing, PRC 3 965 (1992).

2.W.W. Wilson, D.V. Srikantaiah, J.T. Lineberry, and J.J. Lee, "Laser Doppler Measurement in the CFFF Radiant Furnace." AIAA-89-0226, 27th Aerospace Sciences Meeting, Reno, Nevada (1989).

3.W.W. Wilson, D.V. Srikantaiah, W.S. Shepard, and R.L. Cook, "Laser Velocimetry Measurements at the Diffuser Exit of a Coal-Fired MHD Channel." Journal of Propulsion and Power, 4 571 (1988).

4.W.W. Wilson, D.V. Srikantaiah, J.T. Lineberry, and J.J. Lee, "Comparisons of LDV Results with Theoretical Flow Predictions for the CFFF Radiant Furnace." Proceedings of the 27th Symposium on Engineering Aspects of Magnetohydrodynamics UTSI, Tullahoma, Tennessee, 1989, p. 3.4.1.

5.F.Y. Yueh, J.P. Singh, E.J. Beiting, W.S. Shepard, and R.L. Cook, "Recent Results in Applications of CARS to Simultaneous Measurement of Temperature and CO Concentrations in an MHD Environment." Proceedings of the 26th Symposium on Engineering Aspects of Magnetohydrodynamics UTSI, Tullahoma, Tennessee, 1988, p. 6.1.1.

6.J.P. Singh and F.Y. Yueh, "Comparative Study of Temperature Measurement with folded BOXCARS and Collinear CARS." Combust. Flame 89 77 (1992).

7.J.P. Singh, F.Y. Yueh, R.L. Cook, J.J. Lee and J.T. Lineberry, "Comparison of CARS Temperature Profile Measurements with Flow-Field Model Calculation in an MHD Diffuser." Applied Spectroscopy, 46, 1649 (1992).

8.L.R. Hester, and R.L. Cook, "Devices for Maintaining Optical Access in High-Temperature Coal Combustion Environments." Review of Scientific Instruments, 62 624 (1991).

9.R.L. Cook and J.T. Lineberry, "Design and Evaluation of an Optical Port Assembly for the Aerodynamic Duct at the CFFF." Proceedings of the 30th Symposium on Engineering Aspects of Magnetohydrodynamics, Inner Harbor - Baltimore, Maryland, 1992, p. XIII.1.1.

10.Lineberry, J.T., and Schmidt, H.J., "Operation and Performance of the CFFF LMF Upstream Test Train in Early Western

Coal Tests", 30th Symposium on Engineering Aspects of Magnetohydrodynamics, Baltimore, MD, June 1992.

11.F. Durst, "Principles and Practice of Laser Doppler Anemometry," 2nd Edition, Academic Press, New York 1991.

12.O.P. Norton, W.W. Wilson, and R.L. Cook, "A Comparison of Velocity Profile Measurements in the CDIF Diffuser with Flow Field Model Calculations." Proceedings of the 30th Symposium on Engineering Aspects of Magnetohydrodynamics, Inner Harbor - Baltimore, MD, 1992, p. XIII.2.1.

13.E.J. Beiting, "Coherent Interference in Multiplex CARS Measurements: Nonresonant Susceptibility Enhancement due to Laser Breakdown," Appl. Opt. 24, 3010 (1985).

14.P.E. Bengtsson, M. Alden, S. Kroll, and D. Nilsson, "Vibrational CARS Thermometry in Sooty Flames: Quantitative Evaluation of C_2 Absorption Interference." Combust. Flame 82, 199 (1990).

5.J.P. Singh and F.Y. Yueh, "Comparative Study of the Temperature Measurement with Folded BOXCARS and Collinear CARS", Combust. and Flame, 89, 77-94 (1992).

16.C.W. Bouchillon, O.P. Norton, and R.L. Cook, "Optical Diagnostics in Supersonic Plasma Flows - Purging Fluid Effects", AIAA-93-0821, 31st AIAA Aerospace Sciences Meeting, Reno, NV, January 1993.

17.B.J. McBride, et. al. "Computer Program for Calculation of Complex Chemical Equilibrium Composition, Rocket Performance, Incident and Reflected Shocks, and Chapman-Jouquet Detonations", NASA SP-273, 1976.

18.Cline, M.C., "VNAP2: A Computer Program for Computation of Two-Dimensional, Time-Dependent, Compressible, Turbulent Flow", Los Alamos National Laboratory Report LA-8872, August 1981.

19.Liao, Yi-Fu, "Simulation of Starting Transients in the UTSI MHD Generator", Ph.D. Dissertation, The University of Tennessee, March 1983.